Journal of Magnetic Resonance 203 (2010) 1–10

Contents lists available at ScienceDirect

Journal of Magnetic Resonance

journal homepage: www.elsevier.com/locate/jmr

Group epitope mapping considering relaxation of the ligand (GEM-CRL): Including longitudinal relaxation rates in the analysis of saturation transfer difference (STD) experiments

Sebastian Kemper [a,1], Mitul K. Patel [a], James C. Errey [a,2], Benjamin G. Davis [a], Jonathan A. Jones [b], Timothy D.W. Claridge [a,*]

[a] Chemistry Research Laboratory, Department of Chemistry, University of Oxford, Mansfield Road, Oxford OX1 3TA, UK
[b] Oxford Centre for Quantum Computation, Clarendon Laboratory, University of Oxford, Parks Road, Oxford OX1 3PU, UK

ARTICLE INFO

Article history:
Received 30 September 2009
Revised 20 November 2009
Available online 26 November 2009

Keywords:
STD
GEM
GEM-CRL
CORCEMA-ST
TreR
Trehalose
Jacalin

ABSTRACT

In the application of saturation transfer difference (STD) experiments to the study of protein–ligand interactions, the relaxation of the ligand is one of the major influences on the experimentally observed STD factors, making interpretation of these difficult when attempting to define a group epitope map (GEM). In this paper, we describe a simplification of the relaxation matrix that may be applied under specified experimental conditions, which results in a simplified equation reflecting the directly transferred magnetisation rate from the protein onto the ligand, defined as the summation over the whole protein of the protein–ligand cross-relaxation multiplied by with the fractional saturation of the protein protons. In this, the relaxation of the ligand is accounted for implicitly by inclusion of the experimentally determined longitudinal relaxation rates. The conditions under which this "group epitope mapping considering relaxation of the ligand" (GEM-CRL) can be applied were tested on a theoretical model system, which demonstrated only minor deviations from that predicted by the full relaxation matrix calculations (CORCEMA-ST) [7]. Furthermore, CORCEMA-ST calculations of two protein–saccharide complexes (Jacalin and TreR) with known crystal structures were performed and compared with experimental GEM-CRL data. It could be shown that the GEM-CRL methodology is superior to the classical group epitope mapping approach currently used for defining ligand–protein proximities. GEM-CRL is also useful for the interpretation of CORCEMA-ST results, because the transferred magnetisation rate provides an additional parameter for the comparison between measured and calculated values. The independence of this parameter from the above mentioned factors can thereby enhance the value of CORCEMA-ST calculations.

1. Introduction

Detecting protein–ligand interactions is the most important step in structure based drug design. The starting point of novel pharmaceutical drug discovery is often determined through the screening of large compound libraries. The results of these screenings may yield promising lead compounds, the structures of which already provide some information about the required features of a potential new drug. To obtain more precise information and hence enable design of drugs with desired properties, knowledge of the bound ligand conformation together with information on its interaction surface with the protein (the ligand epitope map) is also often essential. In both fields of ligand screening and structure determination of protein–ligand interactions, NMR methods are well established and gaining greater popularity [1,2].

Under the numerous NMR techniques developed, saturation transfer difference (STD) [3] is one such method which has become established for both purposes. The relatively small amount of target protein required for a measurement and the easy application of the technique make it an attractive screening method. Furthermore, the STD technique is a method in which information about the ligand interaction surface with the protein can be gained through definition of a group epitope map (GEM) [4] for the bound ligand. In this, the relative STD enhancements for individual protons within the ligand are interpreted such that the highest enhancement factors are considered to reflect the closest proximity to the protein structure at the binding site. However, this common approach to interpret the STD effects is prone to complication; most notably the relaxation of the ligand protons and the exchange kinetics can influence

* Corresponding author. Fax: +44 1865 285002.
E-mail address: tim.claridge@chem.ox.ac.uk (T.D.W. Claridge).
[1] Present address: Department of Chemistry, University of Cologne, Greinstrasse 4, 50939 Cologne, Germany.
[2] Present address: Heptares Therapeutics, BioPark, Broadwater Road, Welwyn Garden City, Herts AL7 3AX, UK.

1090-7807/$ - see front matter © 2009 Elsevier Inc. All rights reserved.
doi:10.1016/j.jmr.2009.11.015

strongly the epitope map [5]. Krishna and Jayalakshmi [6,7] have addressed this through the application of a complete relaxation and exchange matrix analysis (CORCEMA-ST) for the STD data, a procedure which calculates these influences and is thus better able to provide quantitative interpretation of these data. Whilst reflecting a thorough and comprehensive approach to data analysis, the CORCEMA-ST method necessarily requires a (proposed) structure of the bound protein–ligand complex and detailed knowledge of the ligand in its unbound state to calculate all necessary relaxation parameters. Furthermore, the program also requires input of the molecular correlation times, concentrations and kinetic and thermodynamic parameters of the association equilibrium. Thus, in practice, these requirements can restrict the application of the CORCEMA-ST program; for example, the K_D and in particular the kinetic rates are often unknown and access to the protein (crystal) structure may also not be possible. Indeed, it is often desirable to apply the STD method to investigate the nature of the ligand–protein interaction *because* the protein structure is unknown. One approach to defining a bound ligand conformation when the protein structure itself is known is the use of a simulated annealing algorithm within the CORCEMA-ST program to refine ligand torsion angles and thus to dock the ligand into the protein [6]. Nevertheless, it is clear that the development of a simple and reliable procedure for epitope mapping which corrects the differential relaxation rates within ligands is desirable since such an approach can be employed even when the protein structure is unknown yet the identification of close contacts between protein and ligand is demanded. Furthermore, a GEM derived from the CORCEMA-ST theory can give new insights into the influence of kinetic and relaxation parameters on the observed STD effects. Thus, we undertook to reassess the principles underlying STD measurements and herein propose a simple approach that is easily applied and which is able to yield more precise group epitope maps from experimental STD data without knowledge of protein structure. We term this approach *group epitope mapping considering relaxation of the ligand* (GEM-CRL).

2. Theoretical basis

In this section we briefly review the theoretical basis for the proposed methodology and describe the process leading to its derivation. To begin, we note that it has been common practice to create group epitope maps from STD data by employing relatively short saturation times (1–2 s) to minimise the influence of ligand relaxation and possible cross-relaxation between spins within the ligand [5]. Although the influences are smaller, the observed STD values are still affected by such relaxation processes combined with the exchange kinetics. A more precise and recently used method is to fit the build-up of the STD to an exponential curve and estimate the initial slope [8,9]. This approach is usually done with short saturation times (~0.3 s), meaning the measured STDs are often intrinsically weak and thus more difficult to quantify, so this approach also imposes undesirable experimental consequences and may be time intensive. Additionally, within the early stages of irradiation (e.g. within the first second), the distribution of saturation throughout the protein changes substantially before it reaches the final equilibrium state, as may be shown by CORCEMA-ST calculations. This process might also influence the observed STD factors and especially the build-up slope. We therefore decided to adopt a different approach and concentrate on the saturation equilibrium condition, which is reached by the spins of the ligand after a sufficient protein saturation period (~5 times T_1). This saturation equilibrium is strongly influenced by the relaxation of the ligand, but like in other steady-state NOEs [10] the cross-relaxation between spins can be determined from knowledge of these relaxation sources (Eq. (1a)). In the following, we show that, under appropriate experimental conditions, a slightly modified equation for the steady-state NOE can be employed for STD experiments (Eq. (1b); see below and supporting information also) which more accurately reflects the transfer of magnetisation from protein onto ligand, as required for accurate epitope mapping. Thus:

$$\sigma_{IS} = \frac{f_I\{S\}}{T_1^I}, \quad f_I\{S\} = \frac{I - I_0}{I_0} \tag{1a}$$

$$q \propto \frac{f_{Lf}\{E\}}{T_1^{Lf}}, \quad f_{Lf}\{E\} = \frac{I_{Lf} - I_{0Lf}}{I_{0Lf}}, \quad q = -\sum \sigma_{EL} f_{Eb} \tag{1b}$$

where σ_{IS} represents the cross-relaxation term between spins I and S, $f_I\{S\}$ is the fractional saturation of spin I arising from saturation of spin S (I and I_0 represent the signal intensity of spin I in the presence and absence of S-spin saturation, respectively) and the term $f_{Lf}\{E\}$ is the fractional STD enhancement observed for the free ligand (L_f) on saturation of the protein (again, I_{Lf} and I_{0Lf} represent the signal intensity of free ligand in the presence and absence of protein saturation, respectively). The newly introduced term q is named the '*transferred magnetisation rate*' and is defined as the summation over the whole protein of the protein–ligand cross-relaxation (σ_{EL}) multiplied with the fractional saturation of the protein protons (f_{Eb}) (Eq. (1b)). It is analogous to the cross-relaxation rate between two single protons in classical steady-state NOE experiments and reflects the 'contact' between the whole protein and specific ligand protons. This parameter may be utilised directly for the proposed group epitope mapping (GEM-CRL) protocol because, as we shall demonstrate, it is largely independent of the relaxation of the ligand and of the exchange kinetics.

Instead of using the complete relaxation matrix, we first reduce the matrix to a system (Eq. (2)), in which we have only one spin of the ligand in two different chemical exchange states (bound to the protein and free in solution). The chemical exchange rates k_b (bound) and k_f (free) in Eq. (2) are defined according to the association equilibrium $E_f + L_f \leftrightarrow EL$ so that k_b is identical to the off-rate constant (k_{off}) and k_f is the product of the on-rate constant and equilibrium concentration of the protein/enzyme ($k_{on}[E]$). We also introduce in this step the transferred magnetisation rate q, being defined as having the same sign as the cross-relaxation rates between the protein and the ligand (f_{Eb} is negative). Thus:

$$\begin{aligned} \frac{dI_{Lb}}{dt} &= \rho_{Lb} I_{0Lb} - (k_b + \rho_{Lb}) I_{Lb} + k_f I_{Lf} + q I_{0Eb} \\ \frac{dI_{Lf}}{dt} &= \rho_{Lf} I_{0Lf} - \left(k_f + \rho_{Lf}\right) I_{Lf} + k_b I_{Lb} \end{aligned} \tag{2}$$

in which ρ_{Lb} and ρ_{Lf} represent the relaxation rates of ligand protons when protein-bound and when free in solution, respectively. Assuming saturation equilibrium, both intensity rates in Eq. (2) can be set to zero and the transferred magnetisation rate is constant. The solutions for the intensities of the ligand spins are then readily achieved and after some transformation we obtain for the free ligand:

$$I_{Lf} - I_{0Lf} = \frac{k_b q I_{0Eb}}{k_b \rho_{Lf} + k_f \rho_{Lb} + \rho_{Lb} \rho_{Lf}} \tag{3}$$

STD experiments are performed mainly with systems requiring a rapid on–off equilibrium, which usually dictates that the off-rate (k_b) is far greater than the relaxation of the ligand in the bound complex (ρ_{Lb}). Under these conditions, the $\rho_{Lb}\rho_{Lf}$ term could then be neglected in Eq. (3) since $k_b \rho_{Lf}$ dominates over $\rho_{Lb}\rho_{Lf}$. Further, under conditions of high ligand excess, one may also neglect the $k_f \rho_{Lb}$ term since k_b is approximately the ligand excess times greater than k_f ($k_b/k_f = K_D/[E] = [L]/[EL] \approx [L]_0/[E]_0$). Thus, although the relaxation in the bound state is more rapid than in the free state

($\rho_b > \rho_f$), the $k_b\rho_{Lf}$ term may readily exceed the $k_f\rho_{Lb}$ term for a typical protein–small ligand system if the ligand excess is around 500 or greater (see below).

After including the equilibrium equation for high ligand excess, a simplified equation can be derived for the observed STD effect $f_{Lf}\{E\}$ (Eq. (4); see Supplementary material), which is dependent only upon the relaxation of the free ligand, the initial concentrations of the protein ($[E]_0$) and ligand ($[L]_0$) and the dissociation constant (K_D):

$$f_{Lf}\{E\} \approx \frac{q[E]_0}{\rho_{Lf}(K_D + [L]_0)} \tag{4}$$

It can be concluded from the resulting equation, that at fast exchange equilibrium and high ligand excess, the spins of the ligand behave as if they receive magnetisation from the protein (at a rate reflected in the term q) yet do not relax whilst bound to it. It also tells us that under the chosen conditions, the STD effects are independent of the exchange kinetics and for sufficiently high ligand concentrations ($[L]_0 >> K_D$) they become independent of the thermodynamics; this behaviour was previously observed in the CORCEMA-ST calculations of Krishna et al. [6,11]. If the conditions required for these simplifying approximations are not achieved, it becomes necessary to consider relaxation of both the free and bound forms of the ligand for correct solutions. If not, the total relaxation for the ligand would then be underestimated using the GEM-CRL approach leading to calculated q values that are too low.

We also analysed ligand systems with more than one spin to see if the cross-relaxation will significantly influence the results. We make similar approximations which lead to Eq. (5), which are extended by the different cross-relaxation terms. The additional approximations now contain conditions concerning the cross-relaxation rates between the ligand protons in the free and bound states ($k_b >> |\sigma_{Lb}|$ and $|k_b\sigma_{Lf}| >> |\sigma_{Lb}k_f|$).

$$q \approx \frac{K_D + [L]_0}{[E]_0}\left(\rho_{Lf}f_{Lf}\{E\} + \sum\left(\sigma^i_{Lf}f^i_{Lf}\{E\}\right)\right) \tag{5}$$

In principle, the relaxation parameters ρ and σ can be determined directly through relaxation measurements, although this is rarely undertaken and it is more common to measure the longitudinal relaxation time constants (T_1s). The non-selective T_1 time constant, as measured with the classical inversion-recovery sequence, will be influenced by cross-relaxation, and the reciprocal of this may be used to reflect approximately the sum of the relaxation rates [10]. The resulting equation then consists only of measurable or known parameters (Eq. (6)). The terms for the concentrations in this equation show parallels to the proposed STD amplification factor of Mayer and Meyer [4]

$$q \approx \frac{K_D + [L]_0}{[E]_0}\frac{f_{Lf}\{E\}}{T_1^{Lf}} \tag{6}$$

or

$$q \propto \frac{f_{Lf}\{E\}}{T_1^{Lf}} \tag{7}$$

Thus, if K_D is known, q may be calculated directly, or, more significantly, even if K_D is unknown, the *relative* rates of magnetisation transfer onto individual ligand nuclei (expressed in q) can be determined using the experimentally measured STD enhancements and T_1 values (Eq. (7)). These transferred magnetisation rates reflect the proximity of protein–ligand "contacts" in the bound state much more accurately than the measured STD enhancements alone, since they are (largely) independent of the relaxation of the ligand, which can otherwise have a substantial influence on the magnitude of observed STD effects.

Clearly, for the application of the GEM-CRL methodology it is important that a number of simplifying approximations are fulfilled. The approximations used in these theoretical predictions are validated in the following sections through both computational and experimental data.

3. Results and discussion

3.1. Conditions for applying GEM-CRL

Since a number of approximations were employed in the derivation of the GEM-CRL equation, its application requires that certain experimental conditions can be fulfilled. In total there are four that must be considered: (1) the STD values must be measured under saturation equilibrium conditions, (2) the ligand excess must be high, (3) the exchange (off) rates must be fast relative to ligand relaxation rates in the bound complex, and (4) the measured longitudinal relaxation rates for the ligand must reflect the influence of cross-relaxation within the ligand. Most of these conditions are either typical for the STD method itself, such as the high off-rate, or can be readily determined by the experimental protocol, such as the use of long saturation times and high ligand excess.

To gain a greater understanding of the limits imposed by the theoretical approximations used, and to compare the proposed GEM-CRL approach with the traditional GEM method, we employed a model protein–ligand system for theoretical calculations with CORCEMA-ST. Thus, we were able to compare the GEM-CRL *estimated* values for the protein–ligand transferred magnetisation rates (derived from the computed STD and T_1 values) with the *exact* transferred magnetisation rates calculated from CORCEMA-ST. It is this latter value that truly reflects the proximity of the protein–ligand contact and hence the accurate epitope map. For a clearer distinction of these two values, that resulting from applying GEM-CRL is herein referred to as the q value, while the exact transferred magnetisation rate derived directly from CORCEMA-ST (the summation of the product of cross-relaxation and fraction of protein saturation, Eq. (1b)), is referred to as the *transferred magnetisation rate*. Clearly, for the approximations used in deriving the GEM-CRL approach to be valid, these two values should be similar.

In the model system, the ligand nuclei were arranged such that the T_1 values of the ligand protons in the free state ranged between 0.5 and 3 s (Fig. 1a; see Supporting information also). The protein was sited tight to the ligand (3.0–4.1 Å) and shaped in such a way that the closest contact is in the middle of the ligand (sites 3 and 4) and the furthest on the ends (sites 1 and 6). The relative STD effects cover values typically encountered in STD experiments in the range of 30–100%, as determined by the use of typical STD parameters (K_D = 100 μM, $k_{on} = 10^9\ M^{-1}\ s^{-1}$, τ_c(EL) = 100 ns and 500-fold ligand excess).

The protein protons close to the ligand (grey spheres in Fig. 1a), which do not receive direct irradiation, are all saturated to a similar extent according to the CORCEMA-ST calculations, meaning the transferred magnetisation rates should be the highest onto ligand protons 3 and 4 and should decrease toward the ends of the ligand (protons 1 and 6). The calculated transferred magnetisation rates show this dependency as expected, whereas the direct STD effects possess a significantly different distribution, as can be observed from the GEM at 2 s saturation (Fig. 1b). Protons with high T_1s (3 s) and hence lower relaxation rates can better 'store' the transferred magnetisation and thus show higher STD effects, whilst for those protons with lower T_1s (0.5 s) this is lost due to faster relaxation. A clear example of this is observed for protons 3 and 4 which share similar distances from the proton yet have differing T_1 values (1.2 and 0.5 s, respectively). The GEM shows a good agreement of proton 3 with the relative value of the transferred magnetisation

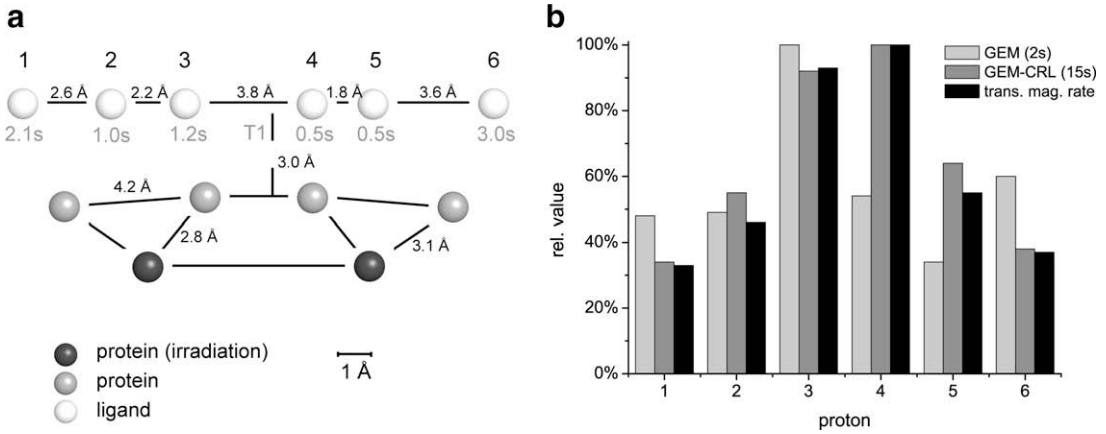

Fig. 1. (a) Hypothetical protein–ligand model used for CORCEMA-ST calculations and (b) the relative values of the computed STD enhancements arising from the GEM (2 s saturation) and GEM-CRL (15 s saturation) protocols and the computed transferred magnetisation rates of the model system. The relative GEM-CRL q values were calculated using Eq. (7); see Supporting information also.

rate, but the GEM value of the faster relaxing proton 4 is only one-half of the transferred magnetisation rate. A similar effect is observable at the fast relaxing proton 5, representing the geminal partner to proton 4. Conversely, proton 6 that is distant from the protein surface exhibits a relative STD value that is too high owing to its relatively slow spin relaxation. These results show that differential relaxation effects may still play a significant role in influencing apparent epitope maps even at relatively short saturation times.

The results from the GEM-CRL procedure provide a more accurate representation of the actual magnetisation transfer rates (Fig. 1b) and demonstrate the method is able to cancel the influence of differential ligand relaxation rates. Most obviously, the results for both protons 4 and 6 have been corrected in GEM-CRL, providing a more accurate epitope map than the classical GEM approach. The only notable deviations for the GEM-CRL data occur for protons 2 and 5. We suggest that these minor deviations appear because of spin diffusion within the ligand whilst this is bound to the protein. Spin diffusion is one effect which still influences the GEM-CRL values, because it is derived from the STD effect, but not the direct transferred magnetisation rates. This may arise in the ligand from protons 3 and 4 which experience high levels of saturation and sit close to protons 2 and 5, respectively.

We extended our analysis by varying the most important parameters of the CORCEMA-ST calculations, including ligand excess, the equilibrium constant, the on-rate and the protein correlation time, to observe the influence on the GEM-CRL values and determine limitations of applicability. When the conditions leave the valid region for the GEM-CRL method, the same two effects could always be observed due to enhanced spin diffusion and relaxation, thus, the q values (calculated via GEM-CRL) of the protons close in space approach each other and all q values decrease. The determined q values are then mostly underestimated relative to the actual transferred magnetisation rates.

Not surprisingly, the influence of the ligand excess proved to be very important, with the q values being dependent on the protein:ligand ratio (Fig. 2a) whereas the actual transferred magnetisation rates, in contrast, remain largely invariant to this. The deviations seen for the GEM-CRL approach at lower ligand excess are caused by the increasing importance of relaxation effects for the ligand in the bound state. Most notably the increasing spin diffusion becomes apparent for the proton pairs 2, 3 (see Supporting information) and for 4, 5 which converge at very low ligand excess. This observation supports the suggested influence of spin diffusion in Fig. 1 and demonstrates that the ligand excess should be set at very high value (at least 200-fold but preferably over 500-fold) to avoid errors. The experimental data described below demonstrate that this approach is practical.

The variation of the dissociation constant K_D in our calculations (Fig. 2b) shows that the transferred magnetisation rate dependence can be loosely categorised for three classes of binder for which the rate is stable over a broad range of K_D: weak (>0.1 M), medium (10 mM–0.1 μM) and strong binding molecules (<1 nM). The lower transferred magnetisation rate with a medium binder can be explained through the withdrawal of magnetisation from the protein surface through the effective transfer onto the ligand. This reduces the protein saturation and therefore also the transferred magnetisation rate. With weak and strong binders the STD effect is very low owing to too short or too long residence times of the ligand, respectively. However, in either case, only a small amount of magnetisation is drawn away from the protein surface and the apparent transferred rates remain high (in this regard, the transferred magnetisation rates for these both states is more of theoretical interest, since despite the high apparent rates, the observable STD factors decrease to become negligible). The GEM-CRL method is able to derive accurate and meaningful q values for the weak and medium binding situations. In the case of stronger binding (<100 nM), the GEM-CRL approach starts to fail. In Fig. 2b it may be observed that with decreasing K_D the spin diffusion increases under strong binding conditions until proton pairs 2, 3 (see Supporting information) and 4, 5 have similar q (GEM-CRL) values and that there is a general decrease of all such q values, although the actual transferred magnetisation rates increase. This is understandable since for the low k_{off} rate associated with the low K_D (as the on-rate is held constant) the approximations implicit in the GEM-CRL method become invalid. In these calculations the on-rate remains diffusion controlled (10^9 M^{-1} s^{-1}); in practice the on-rate may be lower and the limit of the K_D for GEM-CRL applicability will be correspondingly higher. The variation of the on-rate shows how far the GEM-CRL is valid if the association is not diffusion controlled (Fig. 2c). It could be observed that down to 10^7 M^{-1} s^{-1} the GEM-CRL method could be applied reliably but if the rate becomes slower than this, the situation parallels that for the strong binder above. Here again the influence of spin diffusion and decrease of all q values at low on-rates are shown clearly, for a given K_D. Since the K_D and the on-rate correlate with the off-rate (which is the critical parameter) it is therefore not surprising that the GEM-CRL approach started to fail when the off-rate became 100 s^{-1} or lower as these parameters were varied. With these results, it can be concluded that the GEM-CRL method introduces er-

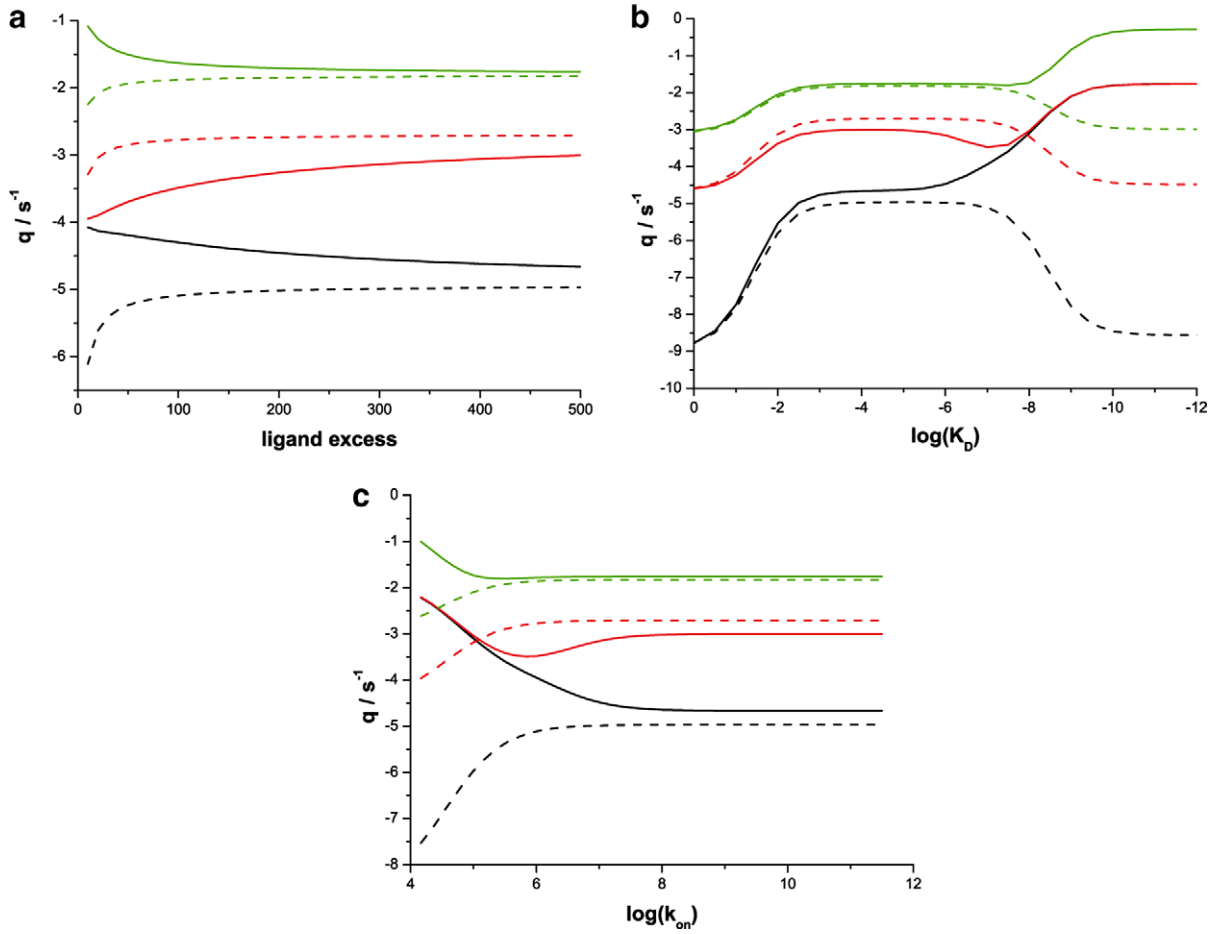

Fig. 2. Calculated transferred magnetisation rates derived from the GEM-CRL analysis (solid lines) or directly from CORCEMA-ST calculations (dashed lines) for the model system described in Fig. 1, shown as a function of (a) ligand excess, (b) dissociation constant and (c) on-rate. Data for three representative protons are illustrated (H4-black, H5-red and H6-green; data for all protons may be found in the Supporting information). The following parameters were used in the CORCEMA-ST calculations with only one being varied for each of the figures: 500-fold ligand excess, K_D = 100 μM, k_{on} = 10^9 M^{-1} s^{-1}, τ_c(EL) = 100 ns.

rors when k_{off} is in the range of 100 s^{-1} down to ca. 0.1 s^{-1}, where STD enhancement can no longer be observed [11,12].

The rotational correlation time of the protein is also an important factor, because all the approximations required for the GEM-CRL approach are relative to relaxation rates and these may be high if using very large or immobilised proteins. The correlation time employed here (100 ns) is relatively high, mimicking a very large protein, and further analysis indicates that only at higher correlation times does the GEM-CRL method introduce errors. We performed calculations with a correlation time of 30 ns, again varying the ligand excess and dissociation constant, which produced similar, or only slightly better, results for the GEM-CRL (see Supporting information). The above mentioned limits should be therefore representative for smaller proteins. We therefore suggest that the method is not applicable for membrane-bound or immobilised proteins but remains valid for protein sizes typically studied by STD.

Finally we note that in these model calculations one parameter only was varied to investigate its influence, whereas on a real system more than one parameter may approach a critical regime. Therefore the GEM-CRL should be used for systems where the necessary conditions are clearly fulfilled and parameters which are adjustable should be set to optimal values by the experimentalist, including high ligand excess and long saturation times. To demonstrate the practical application of the GEM-CRL methodology, we present data on two sugar-binding protein systems. These have been chosen as model systems since the STD method has found widespread application to such complexes, although the approach presented herein would be equally relevant to other ligand complexes.

3.2. Case A: Jacalin

We choose Jacalin, a lectin from jackfruit, to test the GEM-CRL methodology on a real system. The protein is readily available, possesses the necessary size for STD measurements (67 kDa tetramer) and the binding of several sugars has already been investigated, with both crystal structures [13] and dissociation constants [14–16] reported. Jacalin is a protein of interest because it shows binding to carcinoma-related muscins and has mitogenic effect on human $CD4^+$ T-cells [17]. We concentrated our comparisons on two crystal structures (PDB ID: 1JAC and 1WS4) with the ligands methyl α-D-glucopyranoside and methyl α-D-galactopyranoside [14,18]. These two ligands bind with different dissociation constants: methyl α-D-glucopyranoside being a weak binder (K_D = 1.0 mM) [14], while methyl α-D-galactopyranoside binds more strongly (K_D = 25–45 μM) [14–16]. The different binding affinities arise from the loss of two hydrogen bonds with the amino terminus (GLY1), on stereochemical inversion at C4 of the ligand. According to our previous results, both associations should fulfil the conditions of fast equilibrium, provided their on-rates are sufficiently rapid (for example, diffusion controlled).

We measured the STD values for both ligands (separately) at several saturation times with a ligand excess of 500. The STD val-

Table 1
Measured values of the STD effects, the T_1 time constants and measured and calculated values of the transferred magnetisation rates between Jacalin and methyl α-D-glucopyranoside (GYP 502 pocket in PDB structure 1WS4). Concentrations of 5.0 μM Jacalin (20 μM binding pockets) and 10 mM methyl α-D-glucopyranoside were used for the measurement. (Parameters for CORCEMA: K_D = 1 mM, $k_{on} = 10^6\ M^{-1}\ s^{-1}$, τ_c(Jacalin) = 40 ns; essentially identical results were dotained with $k_{on} = 10^9\ M^{-1}s^{-1}$).

	Proton							
	1[a]	2	3	4	5	6S	6R	Me
Experimental								
STD % (2 s)		−0.95	−0.63	−1.37	−0.63	−1.97	−0.93	−0.73
STD % (10 s)		−1.60	−1.09	−2.68	−1.09	−2.21	−0.94	−1.21
T_1/s		2.06	2.82	2.12	1.57	0.75	0.75	1.45
q (GEM-CRL)/s^{-1}		−4.27	−2.13	−6.95	−3.82	−16.32	−6.86	−4.60
Calculated								
q (CORCEMA)/s^{-1}	−6.81	−8.63	−1.03	−5.98	−2.33	−16.49	−7.26	−2.72

[a] Proton 1 was masked by the water resonance.

ues and the corresponding q values from the GEM-CRL analysis (as calculated with eq. 6 above) are then compared with the values calculated from the crystal structure *via* CORCEMA-ST (experimental details may be found in the Supporting information).

From the comparison of measured and calculated q values of the methyl α-D-glucopyranoside/Jacalin system it may be seen that the transferred magnetisation rates derived from the experimental GEM-CRL analysis show very clearly the same ordering as the transferred magnetisation rates calculated for the crystal structure (1WS4), with only the values of the C2 proton showing significant deviation from the overall trend (Table 1 and Fig. 3a). Thus, the GEM-CRL data provide an accurate map of the binding epitope observed in the crystal structure, demonstrating a very good correlation for the methyl α-D-glucopyranoside GYP502 pocket (Fig. 3b). The GEM-CRL is essentially free of spin diffusion artefacts arising from the bound state, where even the closely neighbouring geminal C6 protons show quite different responses. In contrast, the GEM method provides a less good overall correlation; although the 6S proton is correctly predicted to give the greatest STD enhancement, those for other protons, especially 3, 4 and 5, tend to be significantly over estimated and present a somewhat distorted epitope map.

The deviation of the transferred magnetisation rate of the C2 proton is striking and deserves comment. Close inspection of the crystal structure reveals a very close interproton separation between the C2 proton and a *meta*-proton of the protein PHE47 aromatic ring (2.46 Å, Fig. 4); only the distance to a α proton of GLY121 is closer (2.41 Å). This phenyl contact therefore contributes very substantially to the CORCEMA-ST derived transferred magnetisation rate onto C2(H), which is calculated from the static crystal structure. However, in solution one would anticipate this phenyl ring to undergo rotational averaging given that it is not deeply buried within the protein structure and so lead to a greater mean distance to C2(H) and thus a reduced saturation transfer onto this ligand proton. This is indeed reflected in the experimental GEM-CRL data and the deviations for the C2 proton observed in Fig. 3a

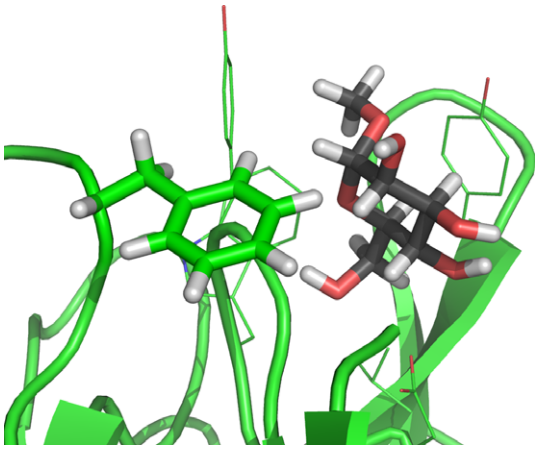

Fig. 4. A region of the crystal structure showing methyl α-D-glucopyranoside in the Jacalin binding pocket (GYP 502 pocket in PDB structure 1WS4). The side chain of PHE47 is seen to be in close contact with both C1(H) and C2(H) in this static representation.

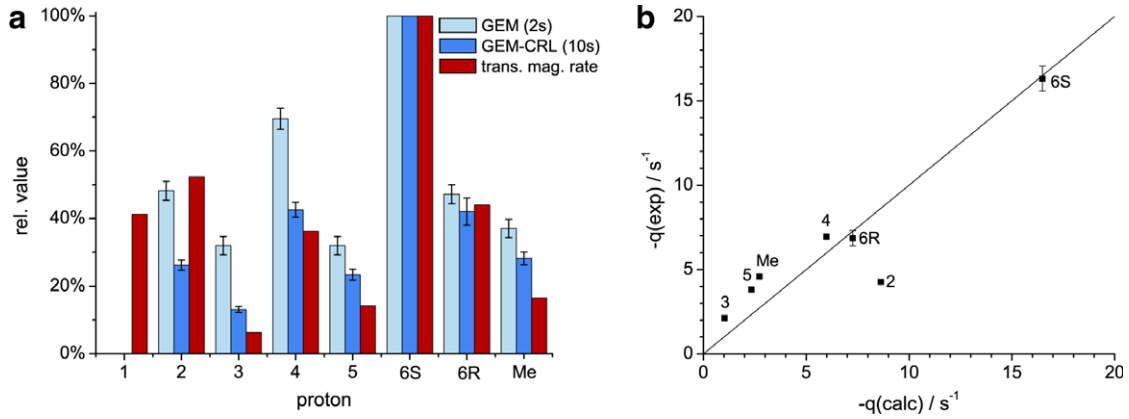

Fig. 3. (a) Relative values of STD enhancements from the experimental GEM and GEM-CRL protocols, and CORCEMA-ST calculated transferred magnetisation rates of methyl α-D-glucopyranoside bound to Jacalin (see Table 1 also). (b) The correlation between q values from CORCEMA-ST calculated transferred magnetisation rates (q_{calc}) and the experimental GEM-CRL method (q_{exp}). (The calculation was performed with the structure 1WS4 for the GYP502 pocket; the solid guide line indicates the ideal correlation. Experimental data for C1(H) could not be obtained because of an overlap with the residual protonated water signal. Error bars are shown only if they exceed the symbol.)

Table 2
Measured values of the STD effects, the T_1 time constants and measured and calculated values of the transferred magnetisation rate between Jacalin and methyl α-D-galactopyranoside. The sample used for the measurements contains 5.0 μM Jacalin (20 μM binding pockets) and 10 mM methyl α-D-galactopyranoside. (Binding pocket of the C chain of PDB structure 1JAC was used. Further parameters for CORCEMA: K_D = 25 μM, k_{on} = 10^6 M^{-1} s^{-1}, τ_c(Jacalin) = 40 ns.)

	Proton					
	1[a]	2, 3	4	5	6	Me
Experimental						
STD % (2 s)		−1.25	−0.86	−1.09	−1.32	−0.87
STD % (10 s)		−2.27	−1.27	−1.48	−1.49	−1.33
T_1/s		2.20	1.51	1.35	0.84	1.38
q (GEM-CRL)/s^{-1}		−5.16	−4.22	−5.50	−8.86	−4.82
Calculated						
q (CORCEMA)/s^{-1}	−9.35	−7.74	−2.90	−3.98	−27.14	−6.04

[a] Proton 1 was masked by the water resonance.

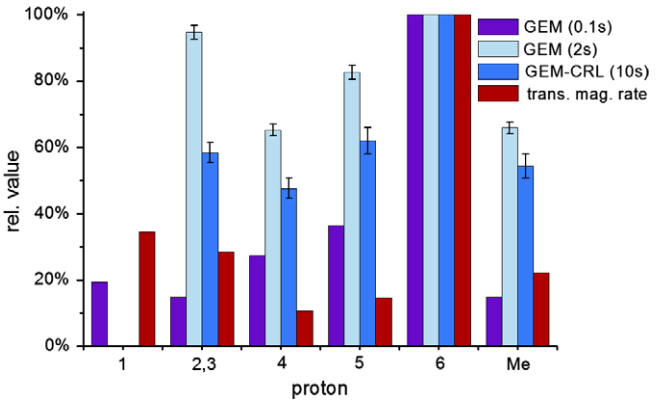

Fig. 6. Calculated initial slope (GEM at 100 ms), experimental GEM (2 s) and GEM-CRL (10 s) values in comparison to the CORCEMA-ST calculated transferred magnetisation rates for methyl α-D-galactopyranoside and Jacalin.

may therefore be attributed to a local difference in the solid-state and solution side-chain conformation within the active site.

The STD spectra of methyl α-D-galactopyranoside are more complex to interpret than those of methyl α-D-glucopyranoside, because discrimination between protons 2 and 3 and between the two 6 protons is not possible, forming two systems of high order. For these discussions, the computed results for these proton pairs have therefore been averaged.

While comparing the measured and calculated transferred magnetisation rates of a CORCEMA-ST calculation using a (diffusion limited) k_{on} rate of 10^9 M^{-1} s^{-1}, it was observed that the GEM-CRL of methyl α-D-galactopyranoside did not show good correspondence with the calculated transferred magnetisation rates for the methyl α-D-galactopyranoside. The general trend that the C6 protons are most saturated was visible (Table 2), but the calculated q value for the C6 protons is far higher in the calculation than estimated through GEM-CRL. Further, the STD effect of the C6 protons yielded from CORCEMA-ST is predicted to be too high (possible rotation of the C(6)H_2 group seems unlikely as this is held by 3 hydrogen bonds; 2 × TRP123 and TYR122).

We hypothesised that slower kinetics were responsible for the failure of the GEM-CRL and for the poorly predicted STD values. We therefore calculated both Jacalin carbohydrate systems again with a reduced on-rate of 10^6 M^{-1} s^{-1}. This change in on-rate had a negligible effect on all values calculated for the methyl α-D-glucopyranoside system (see Supplementary material), but the STD values of the methyl α-D-galactopyranoside, especially that of the C6 protons, changed such that they fitted well to the measured STD data (Fig. 5). This differing response to the change of the on-rate arises due to the different K_D values of these sugars, and in turn to differences in the critical off-rate. An additional calculation with an on-rate of 10^7 M^{-1} s^{-1} shows little difference to 10^9 M^{-1} s^{-1} and that the behaviour changes first at 10^6 M^{-1} s^{-1} (Fig. 5); this corresponds to an off-rate of only 25 s^{-1} and the result fits well within the previously determined k_{off} lower limit of 100 s^{-1} for the validity of the GEM-CRL approach.

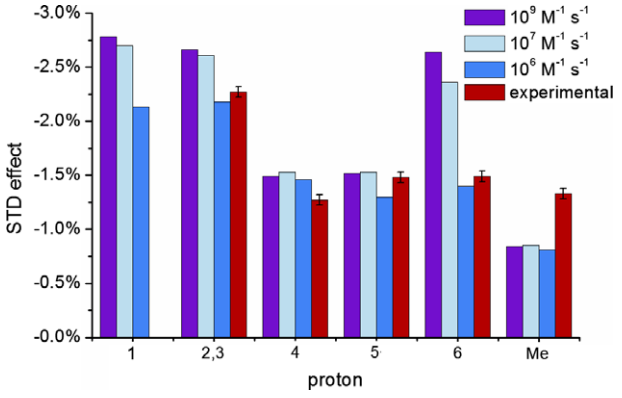

Fig. 5. Comparison of the calculated STD values using different on-rates with the experimental values of methyl α-D-galactopyranoside and Jacalin.

The errors occurring in the GEM-CRL are mainly due to enhanced spin diffusion between the ligand protons, which is not accommodated in the GEM-CRL method. This is observable for the C6 and C5 protons, wherein the q value of the C6 protons is underestimated in favour of C5, which is overestimated.

One caveat of the GEM-CRL method is that its failure may be only anticipated if the off-rate is known or from appropriate CORCEMA-ST calculations, as above. However, any resulting misinterpretation will be influenced only by the enhanced spin diffusion (which will tend to equalise the transferred magnetisation rates, and hence experimental q values, across ligand protons) and by faster spin relaxation (which will mainly influence the absolute magnitudes of the STD values), meaning the overall trend in the epitope map should be still visible (Fig. 6). The GEM-CRL method is not alone with this problem, with other approaches to defining epitope maps also limited by slow exchange kinetics. For example, the experimental GEM at 2 s saturation time shows a similar, but less distinct, profile to that of GEM-CRL, illustrating similar limitations (Fig. 6). We also calculated the STD values at a very low saturation time (100 ms) to assess whether consideration of the initial STD build-up would lead to more reliable predictions [8,9]. The overall profile of this GEM, with low values for all protons except the C6 protons, did fit well with the transferred magnetisation rates, but the ordering of the other protons are again rather poor (Fig. 6). This approach is also experimentally compromised owing to the likelihood of very weak STD enhancements at short saturation times.

3.3. Case B: TreR

The ligand interaction between TreR and trehalose (α-D-glucopyranosyl-(1 → 1)-α-D-glucopyranoside) was chosen as a further example to apply the GEM-CRL method. TreR is a repressor protein, which is involved in the pathway of trehalose utilisation in *Escherichia coli*. It controls the treB/treC operon, expression of which delivers the necessary proteins to phosphorylate trehalose and cleave it to glucose and glucose-6-phosphate. Over these steps *E. coli* can utilise trehalose as sole carbon source at low osmolarity. The repressor activity of TreR is regulated through competition be-

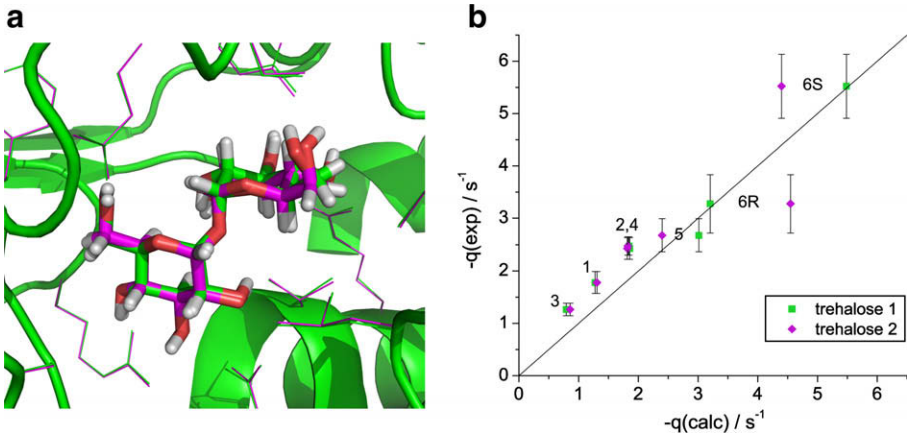

Fig. 7. (a) Superimposed crystal structures of the two binding pockets of the TreR dimer, used for the CORCEMA-ST calculations (trehalose 1 (green): B chain and trehalose residue 316; trehalose 2 (magenta): A chain and trehalose residue 317). (b) Correlation diagram between experimentally measured (GEM-CRL, q_{exp}) and calculated transferred magnetisation rates (q_{calc}) from the two CORCEMA-ST predictions. A sample of 12 μM TreR (24 μM binding pockets) and 20 mM trehalose was used for the measurement. The calculated values of the protons of both rings were averaged due to the symmetrical nature of trehalose. (For interpretation of the references to color in this figure legend, the reader is referred to the web version of this paper.)

tween trehalose-6-phosphate as inducer and trehalose as non-inducer. Fluorescence investigations were able to detect this competitive binding and determine the dissociation constants of both sugars (10 μM for trehalose-6-phosphate, 280 μM for trehalose) [19]. We also observed such competitive binding in STD titration experiments, wherein no STD effects can be observed for trehalose-6-phosphate, while trehalose demonstrates measurable enhancements. The crystal structures of the dimeric TreR with trehalose and trehalose-6-phosphate were studied by Hars et al. [20] and while the structure of TreR with trehalose-6-phosphate was reported, the diffraction data of the corresponding trehalose crystal provided poorer resolution. Hars et al. concluded a structure similar to the TreR/trehalose-6-phosphate complex existed for trehalose, because the comparison of the both datasets showed a good alignment [20], although previously reported fluorescence spectra pointed to differing global conformations [19].

We measured STD spectra for the TreR–trehalose complex and compared them with CORCEMA-ST calculations of the trehalose-6-phosphate crystal structure, in which the phosphate group was removed (Fig 7a; see Supporting information also). This comparison should indicate whether the structures of the TreR complex of trehalose-6-phosphate and trehalose show similarities in solution. A remarkable correlation between the GEM-CRL q values and the calculated transferred magnetisation rates could be observed suggesting strongly that the binding pocket structure in solution of trehalose with TreR must match closely that of the crystal structure of trehalose-6-phosphate (Fig. 7b). Interestingly, the results are dependent on which of the two binding pockets of the dimeric protein complex are used for the CORCEMA-ST calculations. Thus, the calculated q values of the C6 protons differed significantly from the measured values for only one of the binding pockets (A chain/trehalose 2). Indeed the two binding pockets in the crystal structure only differ in the conformation of the C6 moiety of the bound sugar (Fig. 7a), yet the GEM-CRL data appear to be sensitive to this small conformational difference. We suggest that the STD GEM-CRL analysis may therefore provide enhanced detail to the (unpublished) trehalose crystal structure and demonstrates that one of the two bound conformations suggested by the trehalose-6-phosphate crystal structure is much more likely to exist in solution.

The good correlation of the q values and the transferred magnetisation rates indicates that the kinetics are fast enough to fulfil the GEM-CRL condition and hence the off-rate is higher than the previously determined lower limit of 100 s^{-1}. This further suggests that on-rates above 10^6 M^{-1} s^{-1} would be consistent with these data, with the CORCEMA-ST q-calculations showing only minor and negligible variations up to the diffusion limit of 10^9 M^{-1} s^{-1}.

The advantage of the GEM-CRL method is made more apparent when the calculated STD effects are compared with the measured values. The calculated STD values are more disordered than the transferred magnetisation rates because of imprecise prediction of the ligand relaxation in its unbound state (Table 3). Although we choose the conformer of trehalose, which was previously observed in solution [21], the T_1 values calculated by CORCEMA-ST differed from the experimentally determined values. These incorrectly predicted values have a direct influence on the calculated STD results: those protons which have underestimated T_1s also possess underestimated STD values (proton 2–4) while overestimated T_1 values lead to overestimated STD effects (proton 5). This effect of the relaxation of the ligand is cancelled out by the GEM-CRL approach.

The STD results of TreR with trehalose again highlight the different capabilities of the GEM-CRL and GEM approaches for defining accurate epitope maps (Fig. 8). The GEM-CRL procedure reflects the transferred magnetisation rate from protein to ligand, which is dependent only upon the spin diffusion within the protein and the cross-relaxation arising between the protein and the ligand, whereas the traditional GEM approach is further influenced and potentially perturbed by the relaxation of the free ligand itself. In

Table 3
Measured and calculated values of the STD effect, the T_1 time constant and the transferred magnetisation rate between TreR and trehalose. The sample used for the measurements contains 12 μM TreR (24 μM binding pockets) and 20 mM trehalose. (Calculated data for binding pocket of trehalose 1 are presented. Parameters for CORCEMA: K_D = 280 μM, k_{on} = 10^6 M^{-1} s^{-1}, τ_c(Jacalin) = 40 ns.)

	Proton						
	1	2	3	4	5	6S	6R
Experimental							
STD % (2 s)	−0.21	−0.26	−0.20	−0.26	−0.23	−0.20	−0.19
STD % (10 s)	−0.26	−0.37	−0.32	−0.44	−0.27	−0.32	−0.19
T_1/s	1.29	1.34	2.23	1.57	0.89	0.51	0.51
q (GEM-CRL)/s^{-1}	−1.78	−2.43	−1.27	−2.48	−2.68	−5.52	−3.28
Calculated (B chain)							
STD % (2 s)	−0.13	−0.16	−0.10	−0.16	−0.28	−0.27	−0.18
STD % (10 s)	−0.20	−0.25	−0.17	−0.25	−0.36	−0.30	−0.21
T_1/s	1.32	1.26	1.56	1.21	1.17	0.51	0.51
q (CORCEMA)/s^{-1}	−1.28	−1.85	−0.79	−1.84	−3.01	−5.75	−2.94

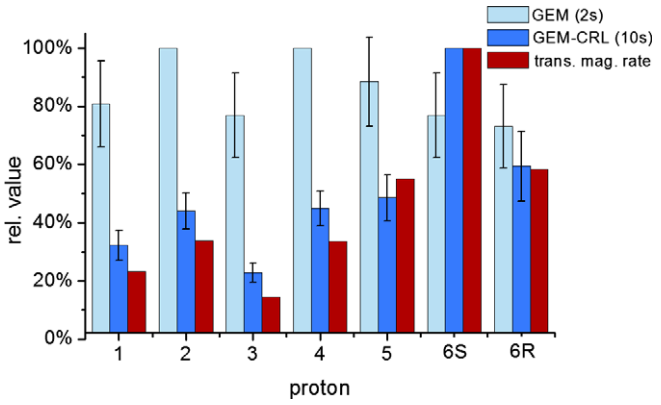

Fig. 8. Comparison of the relative experimental STD or *q* factors for trehalose and TreR determined from the GEM and GEM-CRL protocols respectively, and the transferred magnetisation rates from CORCEMA-ST calculations of the crystal structure (derived from the trehalose-6-phosphate analogue structure).

the system of TreR and trehalose, this may be observed in the high relative STD values of the slowly relaxing protons (proton 2–4), which are at a similar level to both C6 protons although in fact the 6*S* proton sits closer to an irradiated amino acid LEU216 (2.2 Å), as reflected accurately in the GEM-CRL data.

4. Conclusions

The GEM-CRL methodology described herein provides an approach that allows one to define accurate ligand epitope maps from STD data without any requirement for knowledge of the protein structure. The development of the GEM-CRL method was led mainly by our desire to understand the influence of the ligand proton longitudinal relaxation rates on STD spectra. Through the derivation and approximations of the GEM-CRL equation from the relaxation matrix, we were able to demonstrate that one can calculate the transferred magnetisation rate from protein to ligand as a parameter that is independent of the relaxation of the ligand in its unbound state. This then describes the epitope map for the bound ligand complex without perturbation by differential ligand proton relaxation rates. Furthermore, the equation also shows negligible dependence on the kinetic exchange parameters and the relaxation of the ligand in the bound complex under the applied conditions of saturation equilibrium, high ligand excess and fast on–off equilibrium exchange (relative to the spin relaxation rates). Under such conditions, analysis of the relaxation matrix describes a situation in which the ligand gains magnetisation from the protein yet dissociates from it too rapidly to experience significant relaxation in the bound state.

In this work we demonstrate that the theoretical approximations utilised in developing the method can be justified by comparing the GEM-CRL results with those from CORCEMA-ST calculations when the critical parameters are in the usual range for STD measurements. We conclude that the GEM-CRL approach could be used to provide accurate epitope maps under the following conditions:

1. The saturation time should be long enough to achieve saturation equilibrium ($5\times T_1$). Under such condition the STD build-up profile reaches a plateau.
2. The ligand excess should be sufficiently high (ideally $\geqslant$500-fold). When the substance has limited solubility, the ligand excess should be not smaller than 200-fold.
3. The GEM-CRL requires that a fast exchange equilibrium exists between free and bound ligand states, as does STD itself. Strong binding molecules will introduce complicating effects such as spin diffusion in the application of GEM-CRL (as well as in other methods) due to the high lifetime of the complex. In this context, strong binding corresponds to a $K_D < 0.1$–100 μM, dependent upon the ligand on-rate. In the case of diffusion controlled on-rates ($k_{on} \sim 10^9\ M^{-1}\ s^{-1}$) the lower valid K_D limit approaches 0.1 μM.
4. The GEM-CRL should be applied cautiously (or not at all) in situations where the macromolecule experiences extremely long rotational correlation times (slow molecular tumbling), for example membrane-bound or immobilised proteins.

The GEM-CRL method provides not only a map which reflects more accurately the contact surface of the ligand in the pocket, it may be also used in addition to CORCEMA-ST calculations through comparison of respective magnetisation transfer rates. Especially for flexible molecules, where the calculation of proton relaxation rates is complex due to conformational exchange, or for molecules with additional relaxation sources (e.g. solvent interaction) this approach may significantly enhance the accuracy of CORCEMA-ST predictions. The benefit of such a combination is exemplified by the solution of the TreR–trehalose complex described above. This example additionally illustrates the potential application of quantitative, sensitive STD analysis in structural biology wherein STD derived data could be used to resolve ambiguities in crystal structures and explore possible differences between the crystal and solution structures of protein–ligand complexes.

Acknowledgments

The authors gratefully acknowledge financial support from the Deutschen Akademischen Austausch Dienst and the Kölner Gymnasial -und Stiftungsfonds (to S.K.). We are greatly indebted to Prof. N. Rama Krishna, University of Alabama, for making available to us the CORCEMA-ST program. We are also grateful to Prof. Winfried Boos, University of Konstanz, for the gift of plasmid pCYTEXPtreR and to Lucia Primavesi and Matthew Paul, Rothamsted Research, for related discussions. S.K. wishes to thank Prof. A. Berkessel and Dr. N.E. Schlörer for assuring financial support and for constructive discussions.

Appendix A. Supplementary data

Supplementary data associated with this article can be found, in the online version, at doi:10.1016/j.jmr.2009.11.015.

References

[1] J.W. Peng, J. Moore, N. Abdul-Manan, NMR experiments for lead generation in drug discovery, Prog. Nucl. Magn. Reson. Spectrosc. 44 (2004) 225–256.
[2] B. Meyer, T. Peters, NMR spectroscopy techniques for screening and identifying ligand binding to protein receptors, Angew. Chem. Int. Ed. 42 (2003) 864–890.
[3] M. Mayer, B. Meyer, Characterization of ligand binding by saturation transfer difference NMR spectroscopy, Angew. Chem. Int. Ed. 38 (1999) 1784–1788.
[4] M. Mayer, B. Meyer, Group epitope mapping by saturation transfer difference NMR to identify segments of a ligand in direct contact with a protein receptor, J. Am. Chem. Soc. 123 (2001) 6108–6117.
[5] J. Yan, A.D. Kline, H. Mo, M.J. Shapiro, E.R. Zartler, The effect of relaxation on the epitope mapping by saturation transfer difference NMR, J. Magn. Reson. 163 (2003) 270–276.
[6] N.R. Krishna, V. Jayalakshmi, Complete relaxation and conformational exchange matrix analysis of STD-NMR spectra of ligand–receptor complexes, Prog. Nucl. Magn. Reson. Spectrosc. 49 (2006) 1–25.
[7] V. Jayalakshmi, N.R. Krishna, Complete relaxation and conformational exchange matrix (CORCEMA) analysis of intermolecular saturation transfer effects in reversibly forming ligand–receptor complexes, J. Magn. Reson. 155 (2002) 106–118.
[8] M. Mayer, T.L. James, NMR-based characterization of phenothiazines as a RNA binding scaffold, J. Am. Chem. Soc. 126 (2004) 4453–4460.
[9] J. Angulo, I. Díaz, J.J. Reina, G. Tabarani, F. Fieschi, J. Rojo, P. Nieto, Saturation transfer difference (STD) NMR spectroscopy characterization of dual binding

mode of a mannose disaccharide to DC-SIGN, ChemBioChem 9 (2008) 2225–2227.
[10] I. Solomon, Relaxation processes in a system of two spins, Phys. Rev. 99 (1955) 559.
[11] J. Angulo, B. Langpap, A. Blume, T. Biet, B. Meyer, N.R. Krishna, H. Peters, M. Palcic, T.J. Peters, Blood group B galactosyltransferase: insights into substrate binding from NMR experiments, J. Am. Chem. Soc. 128 (2006) 13529–13538.
[12] I. Pérez-Victoria, S. Kemper, M.K. Patel, J.M. Edwards, J.C. Errey, L.F. Primavesi, M.J. Paul, T.D.W. Claridge, B.G. Davis, Saturation transfer difference NMR reveals functionally essential kinetic differences for a sugar-binding repressor protein, Chem. Commun. (2009) 5862–5864.
[13] See PDB entries: 1UGW, 1UGY.
[14] A. Arockia Jeyaprakash, G. Jayashree, S.K. Mahanta, C.P. Swaminathan, K. Sekar, A. Surolia, M. Vijayan, Structural basis for the energetics of jacalin–sugar interactions: promiscuity versus specificity, J. Mol. Biol. 347 (2005) 181–188.
[15] M.V. Sastry, P. Banarjee, S.R. Patanjali, M.J. Swamy, G.V. Swarnalatha, A. Surolia, Analysis of saccharide binding to *Artocarpus integrifolia* lectin reveals specific recognition of T-antigen (beta-D-Gal(1–3)D-GalNAc), J. Biol. Chem. 261 (1986) 11726–11733.
[16] S.K. Mahanta, M.V. Sastry, A. Surolia, Topography of the combining region of a Thomsen–Friedenreich-antigen-specific lectin jacalin (*Artocarpus integrifolia* agglutinin). A thermodynamic and circular-dichroism spectroscopic study, Biochem. J. 265 (1990) 831–840.
[17] S. Kabir, Jacalin: a jackfruit (*Artocarpus heterophyllus*) seed-derived lectin of versatile applications in immunobiological research, J. Immunol. Methods 212 (1998) 193–211.
[18] R. Sankaranarayanan, K. Sekar, R. Banerjee, V. Sharma, A. Surolia, M. Vijayan, A novel mode of carbohydrate recognition in jacalin, a Moraceae plant lectin with a beta-prism fold, Nat. Struct. Biol. 3 (1996) 596–603.
[19] R. Horlacher, W. Boos, Characterization of TreR, the major regulator of the *Escherichia coli* trehalose system, J. Biol. Chem. 272 (1997) 13026–13032.
[20] U. Hars, R. Horlacher, W. Boos, W. Welte, K. Diederichs, Crystal structure of the effector-binding domain of the trehalose-repressor of *Escherichia coli*, a member of the LacI family, in its complexes with inducer trehalose-6-phosphate and noninducer trehalose, Protein Sci. 7 (1998) 2511–2521.
[21] A. Poveda, C. Vicent, S. Penadés, J. Jiménez-Barbero, NMR experiments for the detection of NOEs and scalar coupling constants between equivalent protons in trehalose-containing molecules, Carbohydr. Res. 301 (1997) 5–10.